Liquid-Liquid Phase Transition in Supercooled Yttria-Alumina

Adrian C. Barnes,[1] Lawrie B. Skinner,[1] Philip S. Salmon,[2] Alexei Bytchkov,[3] Irina Pozdnyakova,[4] Thomas O. Farmer,[1] and Henry E. Fischer[5]

[1]*H. H. Wills Physics Laboratory, University of Bristol, Tyndall Avenue, Bristol, BS8 1TL, United Kingdom*
[2]*Department of Physics, University of Bath, Bath, BA2 7AY, United Kingdom*
[3]*European Synchrotron Radiation Facility, 6 rue Jules Horowitz, BP 220, F-38043, Grenoble, France*
[4]*CNRS-CEMHTI, University of Orleans, 1d avenue de la Recherche Scientifique, 45071, Orléans cedex 2, France*
[5]*Institut Laue-Langevin, 6 rue Jules Horowitz, BP 156, F-38042, Grenoble, France*

(Received 13 July 2009; revised manuscript received 5 October 2009; published 23 November 2009)

The structure and thermal characteristics of aerodynamically levitated samples of yttria-alumina in the liquid, supercooled liquid and solid phases were explored in an extensive series of high energy x-ray diffraction, small angle neutron scattering, and pyrometric cooling measurements. Particular focus was placed on the compound $(Y_2O_3)_x(Al_2O_3)_{1-x}$ with $x = 0.2$ for which a liquid-liquid phase transition at a temperature of 1788 K has recently been reported. No structural or thermal signature in support of this metastable phase transition could be found.

DOI: 10.1103/PhysRevLett.103.225702 PACS numbers: 64.70.Ja, 61.05.cp, 61.20.Lc, 64.60.My

First-order liquid-liquid transitions between phases with identical composition but different structures and thermodynamic characteristics provide one of the scenarios for rationalizing the anomalous properties of a wide range of materials such as water [1–5]. A growing body of evidence has been presented in support of liquid-liquid phase transitions, especially from computer simulation [4–7]. However, direct experimental evidence is limited and often disputed. For example, in phosphorus a structural transition occurs at high temperatures and high pressures with a large volume change of 40% that is indicative of a first-order transition between a dense molecular fluid and a polymeric liquid [8–10]. In the case of yttria-alumina, the occurrence of a liquid-liquid phase transition with a volume change of 4% has been inferred from the two-phase glass recovered after the liquid is quenched rapidly from high temperatures [11,12], although the composition range over which this phenomenon occurs, and the experimental conditions required to produce the effect, are not clear [13,14]. In consequence, the direct observation by Greaves *et al.* [15] of a first-order liquid-liquid phase transition at temperature $T_{LL} = 1788$ K in aerodynamically levitated supercooled $(Y_2O_3)_x(Al_2O_3)_{1-x}$ for the composition $x = 0.2$ is a milestone. The evidence in Ref. [15] comprised the measurement, as a function of temperature in the supercooled liquid, of changes in (i) wide angle x-ray scattering (WAXS) data, notably an abrupt shift in the position and intensity of the first diffraction peak, (ii) a rise and fall of the integrated small angle x-ray scattering (SAXS) intensity around a temperature corresponding to the changes observed in the WAXS data, and (iii) the observation of a so-called polyamorphic rotor effect for the levitated samples.

In this Letter we report on extensive high energy x-ray diffraction (HEXD), small angle neutron scattering (SANS) and pyrometry studies of aerodynamically levitated samples of $(Y_2O_3)_x(Al_2O_3)_{1-x}$ $(0.2 \leq x \leq 0.375)$. In view of the observation of a first-order liquid-liquid phase transition by Greaves *et al.* [15] at $x = 0.2$, the focus of attention will be on this composition, henceforth referred to as AY20. HEXD measurements were made for the liquid phase in equilibrium and in the stable supercooled regime at temperatures down to 1573 K, i.e., spanning the reported transition at $T_{LL} = 1788$ K. In addition, time-resolved diffraction patterns were taken of the liquid as it was quenched from different starting temperatures. The new results for AY20 do not support the conclusions drawn in Ref. [15]. Specifically, the HEXD results do not show any sharp changes in structure as the liquid is supercooled, there is no change in the SANS intensity, the pyrometry cooling curves do not show any thermal signature of a first-order liquid-liquid phase transition, and the polyamorphic rotor effect is not associated with a particular temperature such as T_{LL}.

The HEXD measurements were made by mounting a conical nozzle aerodynamic levitation system on beam line ID11 at the European Synchrotron Radiation Facility (ESRF). An incident energy of 101.5 keV was used for which the sample has a small x-ray attenuation coefficient ($\sim$0.2 mm^{-1}) so that scattering comes from the bulk material and any positioning errors will have a minor effect on the measured intensity. The sample composition was carefully controlled [13]. Temperature gradients in the molten spherical samples, of diameter $\simeq$3 mm, were minimized by using two lasers, one directed at the top of the sample and the other directed at the bottom through the nozzle. The incident x-ray beam, of size 400×400 μm, passed through the upper hemisphere of the sample just above its center. A FreLoN 2k16 charge coupled device (CCD) detector was used to collect the data [16] and was set perpendicular to the incident beam at a distance of 160 mm from the sample center. For the time-resolved studies it was operated in a reduced resolution mode in

order to achieve a rate of 30 frames s^{-1}. The centering of the diffraction image on the CCD and the wave vector Q calibration were found by measuring the powder diffraction patterns for crystalline LaB_6 and silicon standards.

For each run, the sample was heated to above the melting point and then cooled, by gradually reducing the laser power, to the starting temperature where it was left to equilibrate for a few minutes. Diffraction patterns with high counting statistics (10 s duration) were then taken for the stable liquid. The time-resolved diffraction patterns were taken in $\simeq$30 ms steps for a total time of $\simeq$5 s as the laser power was instantaneously cut. The cooling curve was simultaneously measured by a pyrometer directed at the top of the sample at an angle of $\simeq$20° to the vertical. The 2D diffraction images were processed using FIT2D [17] and were corrected with dark field images of the same acquisition time before they were reduced to 1D powder patterns. These patterns were then corrected for background scattering and normalized by fitting to the sum of the self and Compton scattering contributions to the x-ray differential scattering cross section [18]. Neutral atom form factors were used for Y, Al, and O.

Figure 1 shows the structure factor $S(Q)$ [18] measured for liquid AY20 at a constant temperature between 2273 and 1573 K. The data sets are remarkable for how little they change over the whole of this 700 K interval. This is emphasized by the insets in Fig. 1 which show (A) details of the first peak in $S(Q)$ and (B) its height as a function of temperature. The results reveal no evidence, within the errors of the correction and normalization procedures, for a step change in the first peak height.

Figure 2 shows the position of the first peak in $S(Q)$ as measured in the time-resolved diffraction experiments as the sample was quenched at an initial rate of between $\approx$250 and 500 K s^{-1} depending on the starting temperature of 1573–2273 K given in Fig. 1. The peak positions obtained for the stable liquids at these starting temperatures are also shown. Over the complete temperature range, a small and steady increase by 0.25 nm^{-1} is observed in the peak position as the liquid is cooled. in Fig. 2 are the points taken from Ref. [15] that were used to signpost a liquid-liquid phase transition. The new results, which straddle the reported value of $T_{LL} =$ 1788 K, therefore show no evidence, within a precision of $< \pm 0.1$ nm^{-1}, for any abrupt change in the first peak position in either the constant temperature or the time-resolved diffraction experiments.

The SANS experiment was made on the D22 beam line at the Institut Laue-Langevin (ILL) using the same levitation system and procedures as for the HEXD measurements. An incident wavelength of 0.45 nm with collimation and sample-to-detector distances of 8 m gave a range $0.08 \leq Q \leq 2$ nm^{-1}. Background and transmission corrections were made using GRASP [19]. The SANS measurements covered temperatures between 1643 and 2023 K in steps of $\approx$20 K. Data were accumulated in 100 s inter-

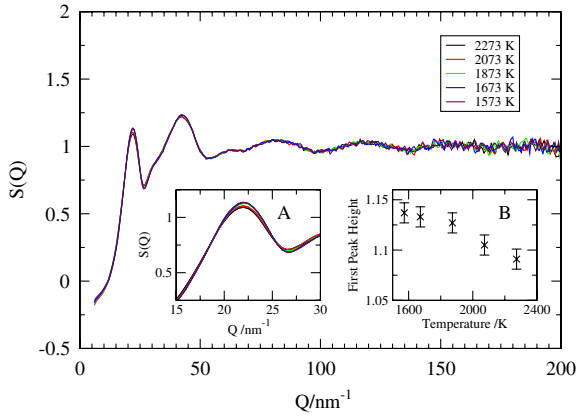

FIG. 1 (color online). The total structure factor $S(Q)$ for liquid AY20 under static conditions at temperatures between 1573 and 2273 K as measured by high energy x-ray diffraction. Inset A shows detail of the first peak in $S(Q)$ at $\sim$22 nm^{-1} and inset B shows the height of this peak as a function of temperature. The melting point of AY20 is about 2123 K [13,22].

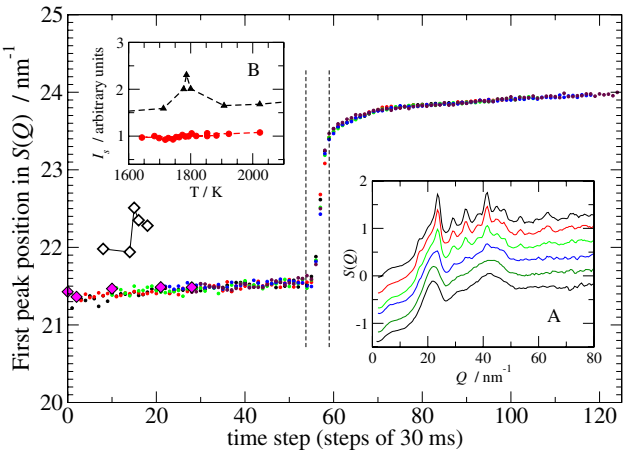

FIG. 2 (color online). The small overlapping points give the first peak position in $S(Q)$ for AY20 as the sample is rapidly quenched from the temperatures shown in Fig. 1, i.e., 2273, 2073, 1873, 1673, or 1573 K. The data were collected in 30 ms time steps and the curves are aligned to the recalescence point at step 56. The filled diamonds show the first peak position in $S(Q)$ for the data shown in Fig. 1 at the starting temperatures of (from left to right) 2273, 2073, 1873, 1673, and 1573 K, respectively. At the point of recalescence the peak transforms to a single Bragg peak at $\simeq$24 nm^{-1}. The open diamonds are the data given in Fig. 3C of Greaves *et al.* [15] for temperatures (from left to right) of $\approx$1900, 1800, 1790, 1780, and 1720 K, respectively. The initial offset between the data sets ($\simeq$0.5 nm^{-1}) is most likely due to use of different methods for determining the peak position. Inset A shows crystallization taking place via the time-resolved $S(Q)$ functions for the steps occurring between the vertical dashed lines in the main panel for a starting temperature of 2273 K. The curves are shifted vertically for clarity of presentation. Inset B shows, as a function of temperature, the integrated SAXS data of Ref. [15] (black triangles) compared to the integrated SANS data of the present work (red circles). The intensity scales I_s are in independent arbitrary units.

vals with a total time per temperature of 1000 s. As shown in Fig. 2, inset B, no change in the SANS signal, and hence the integrated intensity, was observed at any temperature down to the point of recalescence. In particular, no enhancement in the SANS was observed close to the reported liquid-liquid transition at 1788 K.

As shown in Fig. 3, the samples eventually recalesced [13] at a temperature $T_{\mathrm{rec}} = 1473 \pm 15$ K. In all cases the time-resolved diffraction patterns showed that T_{rec} coincides with the onset of crystallization and the time scale (~1 s) for the slow recalescence phenomenon corresponds to the time it takes for the sample to fully crystallize. There is no evidence in Fig. 3 for any phase transition taking place before T_{rec}. A first-order liquid-liquid phase transition at temperature T_{LL} would be noticeable as a marked

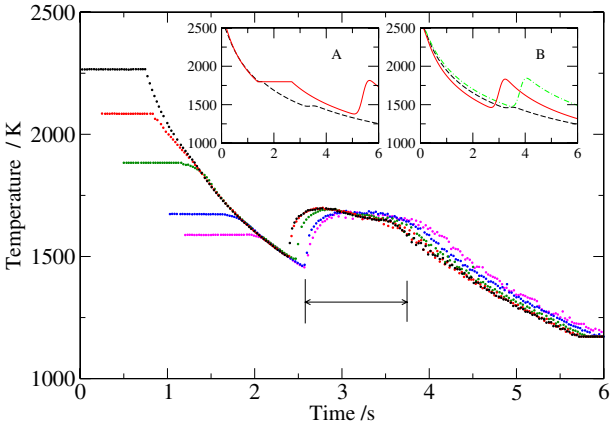

FIG. 3 (color online). The pyrometry traces for AY20 as the sample is quenched from starting temperatures of 2273, 2073, 1873, 1673, or 1573 K. The plots are aligned to the prerecalescence slope and T_{rec} varies by ≃30 K with a tendency for it to decrease with starting temperature. An emissivity correction was not made and it is estimated that the real temperatures are ≈30 K higher [13]. The horizontal bar marks the time it takes for the sample to crystallize as observed in the time-resolved diffraction patterns. Inset A shows, on the same axes, the predicted cooling curve by radiation from 2600 K for an AY20 sample (broken black curve) with $\Delta H_{LL} = 34 \pm 8$ kJ mol^{-1}, $\Delta H_f = 2\Delta H_{LL}$ [15], and $c = 726$ J mol^{-1} K^{-1} as estimated by averaging the c values for YAG ($Y_3Al_5O_{12}$) (=550 J mol^{-1} K^{-1} [22]) and Al_2O_3 (=154 J mol^{-1} K^{-1} [21]) where the molecular unit of AY20 is expressed as $Y_2Al_8O_{15}$. Also shown (solid red curve) is the predicted cooling curve for AY20 using the same model but with ΔH_f increased to 595 kJ mol^{-1} as estimated by averaging the ΔH_f values for YAG and Al_2O_3. The liquid-liquid transition is notable as a plateau on the cooling curve which causes a delay in the time to recalescence. Inset B shows, on the same axes, the cooling curves calculated in the absence of a prerecalescence liquid-liquid transition for AY20 using $\Delta H_f = 2\Delta H_{LL} = 68$ kJ mol^{-1} [15] (broken black curve), for YAG using $\Delta H_f = 516$ kJ mol^{-1} and $c = 550$ J mol^{-1} K^{-1} [20,22] (solid red curve), and for Al_2O_3 using $\Delta H_f = 110$ kJ mol^{-1} and $c = 154$ J mol^{-1} K^{-1} [20,21] (dot-dashed green curve). In A and B the curves were calculated by using the equations given in the text for a sample of 3 mm diameter.

reduction or flattening in the slope of the cooling curve as the sample loses latent heat at constant temperature or, if the sample supercools below T_{LL}, as a recalescence event similar to that observed on crystallization.

To illustrate this point, a simple model for a sphere of mass m cooling by simple black-body radiation at temperature T was used to rationalize the main features of the cooling curves in a semiquantitative way. The radiated power, P, is given by Stefan's law $P = \epsilon\sigma A(T^4 - T_0^4)$ where ϵ is the emissivity (assumed to be unity for simplicity), σ is Stefan's constant, A is the surface area of the sphere, and T_0 is the ambient temperature. In equilibrium P should correspond to the absorbed laser power, in agreement with experiment. When the laser power is cut abruptly the sample temperature will decrease at a rate dT/dt as energy is lost from its surface and Stefan's law can be rewritten as $mc(dT/dt) = \epsilon\sigma A(T^4 - T_0^4)$ where c is the specific heat capacity at constant pressure. This equation may be solved to give the time taken to reach temperature T

$$t(T) = \frac{1}{KT_0^3}\left[-\frac{1}{4}\frac{\ln(T+T_0)}{\ln(T-T_0)} - \frac{1}{2}\tan^{-1}\frac{T}{T_0}\right] + \text{const}, \quad (1)$$

where $K = \epsilon\sigma A/mc$ and the constant may be set according to the boundary conditions to give $t = 0$ for the starting temperature. Equation (1) gives good agreement with the cooling rates observed (before recalescence) for samples of yttrium aluminium garnet (YAG) ($x = 0.375$) and alumina ($x = 0$).

There are two main scenarios if a first-order phase transition occurs at temperature T_p on cooling. First, if the sample does not supercool it will remain at T_p for a time Δt until all the enthalpy for the transition ΔH_p has radiated away, at which point the temperature will again start to fall. By integrating Stefan's law with respect to time and rearranging it follows that $\Delta t = \Delta H_p[\epsilon\sigma A(T_p^4 - T_0^4)]^{-1}$. Alternatively, if the sample does supercool below T_p then the enthalpy for the transition will be released into the sample. If nucleation of the second phase is extremely rapid with a rate much faster than the free cooling rate of the sample then a sudden rise in temperature (the recalescence) will be observed. For instant and complete nucleation the temperature rise ΔT can be calculated from $mc\Delta T = \Delta H_p$ where c now corresponds to the lower temperature phase. This would be observed as an abrupt increase in temperature followed by a cooling curve dependent on the heat capacity of the nucleated phase as typically observed for supercooled liquid alumina. If the nucleation is not, however, instantaneous as in the case of AY20 then the cooling equations need to be solved numerically using a model for the nucleation rate $R(t)$ of the second phase where $-mc(dT/dt) + R(t) = \epsilon\sigma A(T^4 - T_0^4)$. A simple Gaussian model for $R(t)$ of width 0.2 s was used in the present work where $\int_{-\infty}^{\infty} R(t)dt = \Delta H_p$.

According to Ref. [15] the enthalpy change associated with the transition at $T_{LL} = 1788$ K is

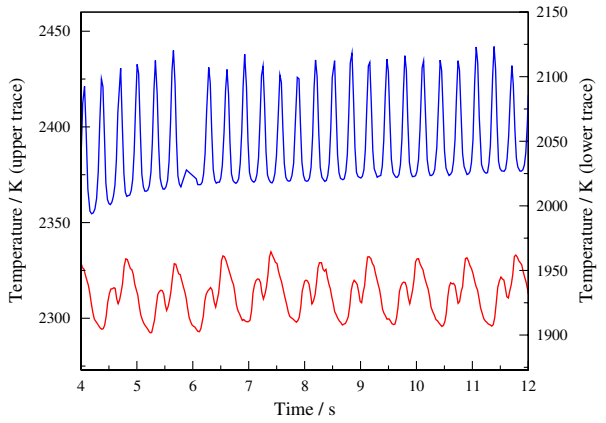

FIG. 4 (color online). Typical examples of the steady oscillations observed at different temperatures for AY20 when the sample is heated by a single laser. The traces show oscillations with an amplitude of ≈60 K occurring at 2373 or 1923 K.

$\Delta H_{LL} = 34 \pm 8\,\mathrm{kJ\,mol^{-1}}$, which corresponds to an entropy change $\Delta S_{LL} = \Delta H_{LL}/T_{LL} = 19 \pm 4\,\mathrm{J\,mol^{-1}\,K^{-1}}$, and $\Delta H_{LL} \simeq \Delta H_f/2$ where ΔH_f is the enthalpy of fusion. Figure 3, inset A, illustrates the predicted effect on the cooling curve for AY20 of this liquid-liquid transition followed by crystallization. Comparison with the main panel in Fig. 3 shows that, although the liquid-liquid transition should be clearly observable as a flattening of the cooling curve before the recalescence event, this does not agree with experiment. In addition, the predicted magnitude of the recalescence event is much smaller than measured, suggesting that the reported value of ΔH_f for AY20 is too small [15]. This is illustrated by Fig. 3, inset B, where the predicted cooling curves and recalescence events for alumina ($\Delta H_f = 109$–$112\,\mathrm{kJ\,mol^{-1}}$, $T_f = 2327$ K [20,21]) and YAG ($\Delta H_f = 420$–$516\,\mathrm{kJ\,mol^{-1}}$, $T_f = 2240$ K [20,22]) are compared with the cooling curve for AY20 as calculated using $\Delta H_f = 2\Delta H_{LL} = 68\,\mathrm{kJ\,mol^{-1}}$ as per Ref. [15]. Unlike the predicted cooling curve for AY20, the curves for alumina and YAG are in good agreement with experiment [13]. As shown by Fig. 3, inset A, an increase of ΔH_f for AY20 to $595\,\mathrm{kJ\,mol^{-1}}$ (obtained by averaging the values for Al_2O_3 and YAG) gives a predicted recalescence event of magnitude that is in much better agreement with experiment and also leads to a much larger signature of the liquid-liquid transition if the relation $\Delta H_f = 2\Delta H_{LL}$ is maintained. Thus, a liquid-liquid transition in AY20 should manifest itself as a prerecalescence event in a measured pyrometer trace even if ΔH_{LL} is as small as $34\,\mathrm{kJ\,mol^{-1}}$. In an extensive number of measurements over a wide range of starting temperatures, with different rates of controlled cooling and for a number of compositions ($0.2 \leq x \leq 0.375$), this characteristic signature of a liquid-liquid transition has not been observed [13].

The value of ΔH_{LL} for AY20 was obtained by Greaves *et al.* [15] by considering a so-called polyamorphic rotor, i.e., a mechanical rotation of the sample initiated by a continual transformation between low and high density liquid phases as the less dense (low temperature) phase rotates to the top of the sample once it has formed after cooling in the levitation gas. This causes oscillations in the observed temperature and the premise is that the rotor effect occurs solely at temperatures bracketing T_{LL}; i.e., it is a signature of the liquid-liquid transition. However, as shown in Fig. 4, it is possible to observe long lived oscillations with similar amplitudes over a *wide range of temperatures* when studying levitated liquids under comparable conditions to Ref. [15]. It is therefore likely that this phenomenon can be attributed to a combination of factors including the rotation and velocity of the levitation gas, the precise size and positioning of the laser spot on the sample sphere, and the properties (e.g., thermal conductivity, viscosity) of the levitated material.

In summary, following an exhaustive set of HEXD, SANS and pyrometry studies we have not been able to find any convincing evidence for a liquid-liquid transition in levitated liquid AY20 as proposed by Greaves *et al.* [15]. Further studies are required to unravel the complexity of behavior for the full yttria-alumina system.

[1] P. G. Debenedetti, *Metastable Liquids* (Princeton Univ. Press, Princeton NJ, 1996).
[2] P. H. Poole *et al.*, Science **275**, 322 (1997).
[3] O. Mishima and H. E. Stanley, Nature (London) **396**, 329 (1998).
[4] P. F. McMillan *et al.*, J. Phys. Condens. Matter **19**, 415101 (2007).
[5] H. E. Stanley *et al.*, Eur. Phys. J. Special Topics **161**, 1 (2008).
[6] S. Sastry and C. A. Angell, Nature Mater. **2**, 739 (2003).
[7] H. M. Gibson and N. B. Wilding, Phys. Rev. E **73**, 061507 (2006).
[8] Y. Katayama *et al.*, Nature (London) **403**, 170 (2000).
[9] G. Monaco *et al.*, Phys. Rev. Lett. **90**, 255701 (2003).
[10] Y. Katayama *et al.*, Science **306**, 848 (2004).
[11] S. Aasland and P. F. McMillan, Nature (London) **369**, 633 (1994).
[12] P. F. McMillan and M. C. Wilding, J. Non-Cryst. Solids **354**, 1015 (2008).
[13] L. B. Skinner, A. C. Barnes, P. S. Salmon, and W. A. Crichton, J. Phys. Condens. Matter **20**, 205103 (2008).
[14] G. N. Greaves *et al.*, J. Non-Cryst. Solids **355**, 715 (2009).
[15] G. N. Greaves *et al.*, Science **322**, 566 (2008).
[16] J.-C. Labiche *et al.*, Rev. Sci. Instrum. **78**, 091301 (2007).
[17] A. P. Hammersley, ESRF, Grenoble, France, Internal Report No. ESRF98HA01T, 1998.
[18] H. E. Fischer *et al.*, Rep. Prog. Phys. **69**, 233 (2006).
[19] C. D. Dewhurst, ILL, Grenoble, France, Internal Report No. ILL03DE01T, 2003.
[20] I.-C. Lin *et al.*, J. Non-Cryst. Solids **243**, 273 (1999).
[21] P.-F. Paradis *et al.*, Jpn. J. Appl. Phys. **43**, 1496 (2004).
[22] O. Fabrichnaya *et al.*, Scand. J. Metall. **30**, 175 (2001).